Ground- and Excited-State Surfaces for the [2+2]-Photocycloaddition of α,β-Enones to Alkenes

Sarah Wilsey,*,‡ Leticia González,⊥,§ Michael A. Robb,§ and K. N. Houk†

Contribution from the Physical and Theoretical Chemistry Laboratory, Oxford University, South Parks Road, Oxford OX1 3QZ, UK, Freie Universität Berlin, Institut für Physikalische und Theoretische Chemie, Takustrasse 3, D-14195, Berlin, Germany, Department of Chemistry, King's College London, Strand, London WC2R 2LS, UK, and Department of Chemistry and Biochemistry, University of California, Los Angeles, California 90095

Received February 23, 2000. Revised Manuscript Received April 19, 2000

Abstract: The potential energy surfaces of the ground state (S_0) and triplet $\pi\pi^*$ (T_1) state for the cycloaddition of acrolein to ethylene have been mapped with ab initio CASSCF calculations and the 6-31G* basis set. The results indicate that transition states on both the triplet and ground-state surfaces play a part in controlling product selectivity, in accord with the experimental results of Weedon and co-workers. The first part of the reaction involves attack of the alkene by either the α- or β-carbon of the triplet cis or trans α,β-enone leading to many different anti and gauche conformations of a triplet biradical intermediate, which then undergoes intersystem crossing to the ground-state surface. The second part of the reaction is controlled by the ground-state surface topology. Ring-closure to products competes with reversion to reactants; anti biradicals have a tendency to dissociate while gauche biradicals favor cyclobutane formation. The addition of the $n\pi^*$ states of acrolein to ethylene has higher barriers than found for the $^3(\pi\pi^*)$ state. α-Attack is strongly disfavored as it involves decoupling electrons, but the barriers for β-attack leading to 1,6-biradicals lie only a few kilocalories per mole higher in energy than those on the $^3(\pi\pi^*)$ surface, suggesting that in more constrained enone systems the $n\pi^*$ states may play a role. Two $^1(n\pi^*)/^3(n\pi^*)/^3(\pi\pi^*)$ crossing regions exist, the first in acrolein itself and the second in the 1,6-biradical region. In the parent system, the biradical crossing points lie some 16 kcal/mol above the $n\pi^*$ minima, such that fast intersystem crossing or internal conversion is more likely to occur before the transition state region. However, in more constrained systems, the reaction could proceed on the $n\pi^*$ states into the biradical region, followed by decay through the four-level degenerate crossing points.

Introduction

The photochemical cycloadditions of α,β-enones to alkenes are important synthetic reactions,[1] and the mechanisms of such processes have been the subject of controversy ever since the first reports by Eaton[2] and Corey[1,3] in the early 1960s. Extensive theoretical and experimental investigations on simple thermal [2+2]-cycloaddition reactions have been reported,[4] and a consistent picture involving biradical intermediates has evolved. However, the experimental results of the photochemically initiated reactions have been more difficult to interpret[5] due to the involvement of one or more excited-state surfaces. Although we[6] and others[7] have carried out detailed computational studies on the [2+2]-photodimerization of ethylene, the inclusion of a C═O chromophore enriches the photochemistry of the system considerably, due to the role of the low-lying $n\pi^*$ singlet and triplet states in acrolein.[8]

One of our groups recently reported a UHF study of the regioselectivity of photocycloadditions of triplet acrolein to a variety of substituted alkenes and showed that in cases where cyclization is fast relative to reversion of the biradical intermediate to reactants, the rates of initial bond formation determine the product regioselectivity.[9] However, Weedon and others have proposed that the rate of cyclization of the biradical, rather than the rate of formation, controls regioselectivities.[10] We have examined the ground and excited states in more detail using CASSCF techniques, and have explored the factors that control product formation in these systems. The potential surfaces for

‡ Oxford University.
⊥ Freie Universität Berlin.
§ King's College London.
† University of California.

(1) It has been used as a key step in natural product synthesis; see, for example: Corey, E. J.; Bass, J. D.; LeMahieu, R.; Mitra, R. B. *J. Am. Chem. Soc.* **1964**, *86*, 5570.

(2) (a) Eaton, P. E.; Hurt, W. S. *J. Am. Chem. Soc.* **1966**, *88*, 5038. (b) Eaton, P. E. *J. Am. Chem. Soc.* **1962**, *84*, 2454.

(3) Corey, E. J.; Mitra, R. B.; Uda, H. *J. Am. Chem. Soc.* **1964**, *86*, 485.

(4) (a) Roberts, J. D.; Sharts, C. M. *Org. React.* **1962**, *12*, 1. (b) Bartlett, P. D. *Q. Rev. J. Chem. Soc.* **1970**, *24*, 473. (c) Hoffman, R.; Swaminathan, S.; Odell, B. G.; Gleiter, R. *J. Am. Chem. Soc.* **1970**, *92*, 7091. (d) Maier, W. F.; Lau, G. C.; McEwen, A. B. *J. Am. Chem. Soc.* **1985**, *107*, 4724. (e) Duran, R.; Bertran, J. *J. Mol. Struct.* **1984**, *107*, 239. (f) Segal, G. A. *J. Am. Chem. Soc.* **1974**, *96*, 7892. (g) Burke, L. A.; Leroy, G. *Bull. Soc. Chim. Belg.* **1979**, *88*, 379. (h) Bernardi, F.; Bottoni, A.; Robb, M. A.; Schlegel, H. B.; Tonachini, G. *J. Am. Chem. Soc.* **1985**, *107*, 2260. (i) Huisgen, R. *Acc. Chem. Res.* **1977**, *10*, 117. (j) Huisgen, R. *Acc. Chem. Res.* **1977**, *10*, 199. (k) Okado, T.; Yamaguchi, K.; Fueno, T. *Tetrahedron* **1974**, *30*, 2293. (l) Inagaki, S.; Fujimoto, H.; Fukui, K. *J. Am. Chem. Soc.* **1975**, *97*, 6108. (m) Wright, J. S.; Salem, L. *J. Am. Chem. Soc.* **1972**, *94*, 322. (n) Borden, W. T.; Davidson, E. R. *J. Am. Chem. Soc.* **1980**, *102*, 5409. (o) Doubleday, C.; McIver, J. W.; Page, M. J. *J. Am. Chem. Soc.* **1982**, *104*, 3768. (p) Doubleday, C.; Camp, R.; King, H. F.; McIver, J. W.; Mullally, D.; Page, M. J. *J. Am. Chem. Soc.* **1984**, *106*, 447.

(5) For a recent review see: Schuster, D. I.; Lem, G.; Kaprinidis, N. A. *Chem. Rev.* **1993**, *93*, 3.

(6) Olivucci, M.; Ragazos, I.; Bernardi, F.; Robb, M. A. *J. Am. Chem. Soc.* **1993**, *115*, 3710.

(7) Doubleday, C., Jr. *J. Am. Chem. Soc.* **1993**, *115*, 11968.

(8) Reguero, M.; Olivucci, M.; Bernardi, F.; Robb, M. A. *J. Am. Chem. Soc.* **1994**, *116*, 2103.

(9) Broeker, J. L.; Eksterowicz, J. E.; Belk, A. J.; Houk, K. N. *J. Am. Chem. Soc.* **1995**, *117*, 1847.

10.1021/ja0006595 CCC: $19.00
Published on Web 06/03/2000

Scheme 1

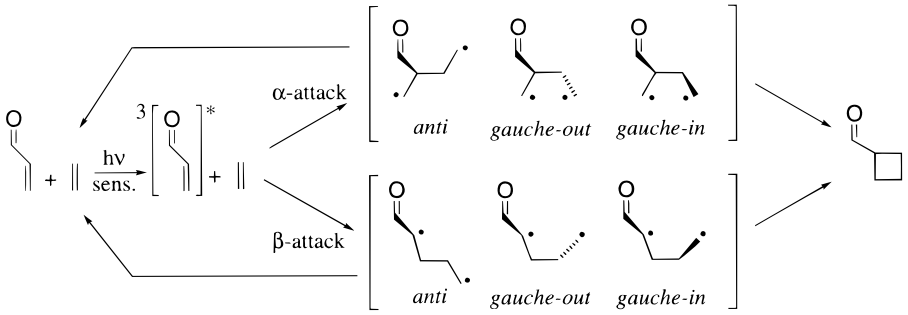

the [2+2]-photocycloaddition of acrolein to ethylene are established in this work. Our central objective is to explore the interplay between the $^3(\pi\pi^*)$ and ground-state surfaces, examining the various conformations via which the reaction can occur, and investigating the competition between ring-closure and reversion from the biradicals on the ground-state surface. The significance of the $n\pi^*$ surfaces and regions of the potential energy surface where $^1(n\pi^*) \rightarrow {}^3(\pi\pi^*)$ intersystem crossing and $^3(n\pi^*) \rightarrow {}^3(\pi\pi^*)$ internal conversion can occur are also investigated.

Background

The photochemical [2+2]-cycloadditions of enones to alkenes involve the initial attack of the excited state α,β-enone on the ground-state alkene (Scheme 1). The photophysics (fluorescence and phosphorescence) of α,β-enones and the lifetimes of the biradical intermediates formed are both very sensitive to the polarity of the solvent and to the acyclic or cyclic nature of the enone used.[11] Acyclic enones have a tendency to relax to the ground-state surface via ultrafast intersystem crossing before they have time to react. On the other hand, the photochemistry of enones seems to be insensitive as to whether the excited enone is obtained by direct irradiation or triplet sensitization, indicating a common mechanism from the $^3(\pi\pi^*)$ and $^1(n\pi^*)$ surfaces.

Early studies[12] based on triplet sensitization and quenching techniques concluded that enone photocycloadditions to alkenes proceed exclusively via the lowest enone triplet excited state,[13] later concluded to be the $\pi\pi^*$ state on the basis of spectroscopic studies on steroidal enones and calculations of the energies of relaxed $n\pi^*$ and $\pi\pi^*$ states.[14] This was confirmed in subsequent studies by Schuster using time-resolved photoacoustic calorimetry (PAC)[15] and transient absorption spectroscopy (TAS).[16] The lifetimes of the triplet biradicals are between 15 and 900 ns, with energies in the range 30−60 kcal/mol above the ground-state reactants.[15,16]

The PAC and TAS results suggest that the triplet states of steroidal and fused-ring enones are essentially planar (long lifetimes, large S_0-T_1 energy gaps), while simple cyclohexenones give highly twisted excited states (short lifetimes, small S_0-T_1 energy gaps). Erickson and Kahn reported calculations that predicted that the twisted $\pi\pi^*$ state gave bond-formation at the β-carbon of the acrolein.[17] The resulting biradical is stabilized due to radical delocalization onto the carbonyl moiety at one center. Both the biradical and the transition state leading to it are more stable than the species formed by α-attack.

Much attention has been focused on both the stereochemical and regiochemical aspects of reactions with substituted alkenes, that is the formation of head-to-head (HH) versus head-to-tail (HT) adducts.[5] HH adducts are those which form with the substituted alkene carbon adjacent to the α-carbon of the enone in the cyclobutane ring, while HT adducts form with the substituted alkene carbon adjacent to the β-carbon of the enone. The photocycloadditions of 2-cyclohexenone to simple alkenes give both HH and HT products; the ratio of HH versus HT adducts depends on whether the alkene is electron-donating or electron-withdrawing.[2] Corey hypothesized that the polarization of the $n\pi^*$ state controls regioselectivity.[2] Nowadays it is generally believed that the ratio of products is related to the barrier heights on the $^3(\pi\pi^*)$ surface leading to the respective 1,4-biradicals.[9] The computed (PMP3/6-31G*//UHF/3-21G) preference for the formation of HH versus HT adducts in the addition of acrolein to substituted alkenes was compared with experimentally determined rates for cyclohexenone addition to the respective alkene, and the computed trends agreed qualitatively with experiment.[9] It was suggested that the enone triplet might be considered to be a nucleophilic alkyl radical at the β-carbon linked to an electrophilic acyl radical at the α-carbon.[9] As the alkene nucleophilicity increases, the preference for attack at the electrophilic α-carbon increases, whereas with electron-deficient or electrophilic alkenes, reaction at the β-carbon is favored. In this way the polarity of the alkene directs the attack of the triplet enone and thus determines the regioselectivity of the reaction.[9]

However, radical trapping experiments of Weedon have suggested that the ratio of HH:HT triplet biradicals is sometimes *not* reflected in the HH:HT ratio of the products formed subsequently.[10] This implies that not all the biradicals formed go on to form products, indicating the existence of a reversion reaction back to reactants that can compete effectively with ring-closure. Weedon attributes product selectivity to this competition between ring-closure and fragmentation back to reactants. We will show that both the triplet-state and ground-state surface

(10) (a) Hastings, D. J.; Weedon, A. C. *J. Am. Chem. Soc.* **1991**, *113*, 8525. (b) Andrew, D.; Hastings, D. J.; Oldroyd, D. L.; Rudolph, A.; Weedon, A. C.; Wong, D. F.; Zhang, B. *Pure Appl. Chem.* **1992**, *64*, 1327. (c) Maradyn, D. J.; Sydnes, L. K.; Weedon, A. C. *Tetrahedron Lett.* **1993**, *34*, 2413. (d) Maradyn, D. J.; Weedon, A. C. *Tetrahedron Lett.* **1994**, *35*, 8107. (e) Andrew, D.; Hastings, D. J.; Weedon, A. C. *J. Am. Chem. Soc.* **1994**, *116*, 10870. (f) Maradyn, D. J.; Weedon, A. C. *J. Am. Chem. Soc.* **1995**, *117*, 5359. (g) Krug, P.; Rudolph, A.; Weedon, A. C. *Tetrahedron Lett.* **1993**, *34*, 7221. (h) Hastings, D. J.; Weedon, A. C. *Tetrahedron Lett.* **1991**, *32*, 4107. (i) Andrew, D.; Weedon, A. C. *J. Am. Chem. Soc.* **1995**, *117*, 5647.

(11) (a) Schuster, D. I. In *Rearrangements in Ground and Excited States*; de Mayo, P., Ed.; Academic Press: London, 1980; Vol. 3, pp 167−279. (b) Schuster, D. I. In *The Chemistry of Enones*; Patai, S., Rappoport, Z., Eds.; John Wiley and Sons: Chichester, UK, 1989; Vol. 2, pp 693−756.

(12) (a) Lam, E. Y. Y.; Valentine, D.; Hammond, G. S. *J. Am. Chem. Soc.* **1967**, *89*, 3482. (b) Ruhlen, J. L.; Leermakers, P. A. *J. Am. Chem. Soc.* **1967**, *89*, 4944. (c) Chapman, O. L.; Kocj, T. H.; Klein, F.; Nelson, P. J.; Brown, E. L. *J. Am. Chem. Soc.* **1968**, *90*, 1657.

(13) de Mayo, P. *Acc. Chem. Res.* **1971**, *4*, 41.

(14) Devaquet, A. *J. Am. Chem. Soc.* **1972**, *94*, 5160.

(15) (a) Schuster, D. I. *Photochem. Photobiol.* **1990**, *52*, 645. (b) Schuster, D. I. *J. Am. Chem. Soc.* **1993**, *115*, 3324.

(16) Schuster, D. I. *J. Am. Chem. Soc.* **1991**, *113*, 6245.

(17) Erickson, J. A.; Kahn, S. D. *Tetrahedron* **1993**, *43*, 9699.

topologies play key roles in determining the product distribution in these systems.

Although it is generally agreed that in most cases the enone−alkene cycloaddition proceeds via the enone $\pi\pi^*$ triplet state, in some special cases (such as in rigid enones) the $n\pi^*$ triplet state may be close or even lower in energy than the $\pi\pi^*$ triplet state. Solvent effects and substituents can also change the ordering of the energy levels. In these cases it is not so easy to predict the state that the reaction will take place through. In addition, the photocycloaddition can occur on both direct and triplet-sensitized photolysis. Therefore a study of reactions initiated on the $^3(\pi\pi^*)$, $^3(n\pi^*)$, and $^1(n\pi^*)$ surfaces has been carried out.

Methodological and Computational Details

All the computations have been performed using the complete active space (CAS) SCF procedure and the standard 6-31G* basis set available in GAUSSIAN 94.[18] CASSCF was chosen as it allows for the balanced representation of several states simultaneously and in this work we are interested in three excited states ($^3(\pi\pi^*)$, $^3(n\pi^*)$, and $^1(n\pi^*)$) and the ground-state surface. CASSCF includes nondynamic correlation energy and thus near degeneracy effects and homolytic bond cleavage are correctly treated. However, it does not include dynamic correlation, which means that biradicaloid structures are more stable than they should be relative to zwitterionic species. However, the central arguments in this paper are focused in the biradical regions so dynamic correlation effects can be safely neglected.

The active space used for the geometry optimizations of the structures on the $^3(\pi\pi)$ and ground-state surface contained six electrons in six orbitals, namely the six π orbitals in the reactants. The orbitals change during the course of the reaction; two of the π orbitals become the σ and σ^* orbitals of the first bond formed in the biradical intermediate, and two more become the σ and σ^* orbitals of the second bond in the cyclobutane product. Analytical frequency calculations were used to confirm the nature of each point located and to compute zero-point energy corrections.

Some structures were also optimized on the $^3(n\pi^*)$ surface. The active space at these points also contained six electrons in six orbitals, but included the n orbital on the acrolein oxygen instead of the carbonyl π orbital. These structures were reoptimized in a CAS(8,7) active space containing both the n and π orbitals where possible, otherwise single-point energies were computed in the larger active space using state-averaged orbitals weighted equally between the two states. The $^1(n\pi^*)$ surface was found to have a very similar surface topology to the $^3(n\pi^*)$ surface. Geometry optimizations proved difficult on the $^1(n\pi^*)$ surface due to problems converging the energy; therefore, CAS(8,7) single-point energies computed at the $^3(n\pi^*)$ optimized geometries are given instead.

The geometry optimizations were carried out using redundant internal coordinates.[19] At a few geometries the forces converged but the predicted displacements did not. This occurs when the surfaces are very flat along a particular coordinate (typically a methylene rotation) and results from a combination of bad updating of an approximate Hessian during the optimization procedure and an eigenvalue in the Hessian that is nearly zero.

Conical intersections were optimized using the algorithm in GAUSSIAN 94 which optimizes the lowest energy point on an $(n-2)$-dimensional conical intersection hyperline.[20] These features have been discussed extensively in the literature, and further details can be found in ref 21. The spin−orbit coupling calculations were carried out using the code implemented in GAUSSIAN 94 which uses a one-electron approximation for the spin−orbit coupling operator with the effective nuclear charges of Koseki et al (C: 3.6, O: 5.6).[22]

Table 1. Energies Computed at the CAS(6,6)/6-31G* Level for the Addition of *s-trans*-Acrolein to Ethylene

structure	figure no.	state	E_{rel}, kcal/mol	ZPE, kcal/mol	E_{rel} + ZPE, kcal/mol
s-trans reactants[a]		S_0	−60.0	74.1	−57.4
		$^3(\pi\pi^*)$	29.5		
s-trans triplet min[a]		$^3(\pi\pi^*)$	0.0	71.5	0.0
cis-formylcyclobutane		S_0	−63.5[b]	80.3	−54.7
			−63.6[b]	80.3	−54.8
trans-formylcyclobutane		S_0	−63.6	80.3	−54.8
α-attack					
anti TS	1a	$^3(\pi\pi^*)$	18.5	73.0	20.0
gauche-out TS	1b	$^3(\pi\pi^*)$	18.5	73.0	20.0
gauche-in TS	1c	$^3(\pi\pi^*)$	18.4	73.0	19.9
anti min	2a	$^3(\pi\pi^*)$	−5.0	74.7	−1.8
		S_0	−5.0		
gauche-out min	2b	$^3(\pi\pi^*)$	−4.9	74.8	−1.6
		S_0	−4.6		
gauche-in min	2c	$^3(\pi\pi^*)$	−3.9	74.6	−0.8
		S_0	−4.6		
anti min (CH_2 twist)	2d	$^3(\pi\pi^*)$	−4.3	74.6	−1.2
		S_0	−6.7		
gauche-out min (CH_2 twist)	2e	$^3(\pi\pi^*)$	−4.8	74.8	−1.5
		S_0	−4.6		
gauche-in min (CH_2 twist)	2f	$^3(\pi\pi^*)$	−4.2	74.7	−1.0
		S_0	−4.3		
anti min	4a	S_0	−7.7	75.2	−4.0
gauche-out min	4b	S_0	−5.3	74.7	−2.1
gauche-in min	4c	S_0	−5.1	74.7	−1.9
anti TS	4d	S_0	−7.4	74.7	−4.2
gauche-out TS	4e	S_0	−4.2	74.3	−1.4
gauche-in TS	4f	S_0	−4.4	74.3	−1.6
gauche-out closure TS	6a	S_0	−4.1[c]	73.8	−1.8
gauche-in closure TS	6b	S_0	−3.0[c]	73.4	−1.1
gauche-out/anti TS	6c	S_0	−4.0	74.9	−0.6
gauche-in/anti SOSP	6d	S_0	−3.4[c]	74.3	−0.6
gauche-out/anti TS	6e	$^3(\pi\pi^*)$	−1.5	74.9	1.9
gauche-in/anti TS	6f	$^3(\pi\pi^*)$	−0.4	74.9	3.0
β-attack					
anti-anti TS	1d	$^3(\pi\pi^*)$	14.6	73.3	16.4
anti-gauche TS	1e	$^3(\pi\pi^*)$	14.6	73.3	16.4
syn-anti TS	1f	$^3(\pi\pi^*)$	15.5	73.5	17.5
syn-gauche TS	1g	$^3(\pi\pi^*)$	15.3	73.6	17.4
anti min	3a	$^3(\pi\pi^*)$	−15.2	75.8	−10.9
		S_0	−16.0		
gauche-in min	3b	$^3(\pi\pi^*)$	−15.3	76.0	−10.8
		S_0	−14.9		
gauche-out min	3c	$^3(\pi\pi^*)$	−14.9	75.9	−10.5
		S_0	−15.1		
anti min	5a	S_0	−16.8	76.1	−12.2
gauche-in min	5b	S_0	−15.2	75.8	−10.9
gauche-out min	5c	S_0	−15.5	75.9	−11.1
anti TS	5d	S_0	−14.4	75.5	−10.4
gauche-in TS	5e	S_0	−12.1	75.2	−8.4
gauche-out TS	5f	S_0	−12.1	75.2	−8.4
gauche-in closure TS	7a	S_0	−14.6	75.3	−10.8
gauche-out closure TS	7b	S_0	−14.7	75.9	−10.3
gauche-in/anti TS	7c	S_0	−13.6	75.9	−9.2
gauche-out/anti TS	7d	S_0	−13.2	75.9	−8.8
gauche-in/anti TS	7e	$^3(\pi\pi^*)$	−11.5	75.9	−7.1
gauche-out/anti TS	7f	$^3(\pi\pi^*)$	−11.7	75.8	−7.4

[a] Energies include acrolein and ethylene. [b] Different energies correspond to using two possible active spaces. [c] Displacements not converged.

(18) Gaussian 94 (Revision A.1), Frisch, M. J.; Trucks, G. W.; Schlegel, H. B.; Gill, P. M. W.; Johnson, B. G.; Robb, M. A.; Cheeseman, J. R.; Keith, T. A.; Peterson, G. A.; Montgomery, J. A.; Raghavachari, K.; Al-Laham, M. A.; Zakrzewski, V. G.; Oriz, J. V.; Foresman, J. B.; Cioslowski, J.; Stefanov, B. B.; Nanayakkara, A.; Challacombe, M.; Peng, C. Y.; Ayala, P. Y.; Chen, W.; Wong, M. W.; Andres, J. L.; Replogle, E. S.; Gomperts, R.; Martin, R. L.; Fox, D. J.; Binkley, J. S.; Defrees, D. J.; Baker, J.; Stewart, J. P.; Head-Gordon, M.; Gonzalez, C.; Pople, J. A., Gaussian, Inc.: Pittsburgh, PA, 1995.

(19) Peng, C. Y.; Ayala, P. Y.; Schlegel, H. B. *J. Comput. Chem.* **1996**, *17*, 49 and references therein.

(20) Bearpark, M. J.; Robb, M. A.; Schlegel, H. B. *Chem. Phys. Lett.* **1994**, *223*, 269.

(21) (a) Klessinger, M. *Angew. Chem., Int. Ed. Engl.* **1995**, *34*, 549. (b) Bernardi, F.; Olivucci, M.; Robb, M. A. *Chem. Soc. Rev.* **1996**, *25*, 321 and references therein.

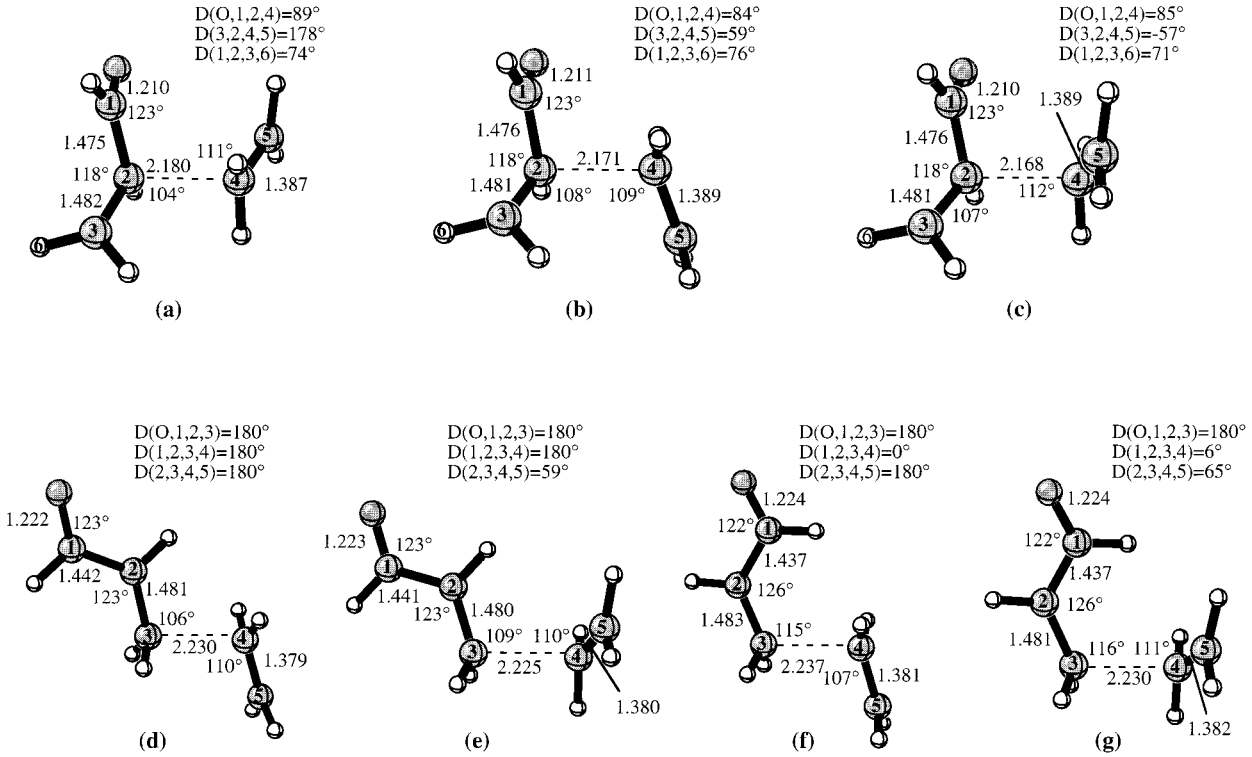

Figure 1. CASSCF(6,6)/6-31G* optimized transition structures for attack of $^3(\pi\pi^*)$ *s-trans*-acrolein on ethylene (bond lengths in Å and angles in deg): (a) *anti* transition structure for α-attack; (b) *gauche-out* transition structure for α-attack; (c) *gauche-in* transition structure for α-attack; (d) *anti-anti* transition structure for *β*-attack; (e) *anti-gauche* transition structure for *β*-attack; (f) *syn-anti* transition structure for *β*-attack; and (g) *syn-gauche* transition structure for *β*-attack.

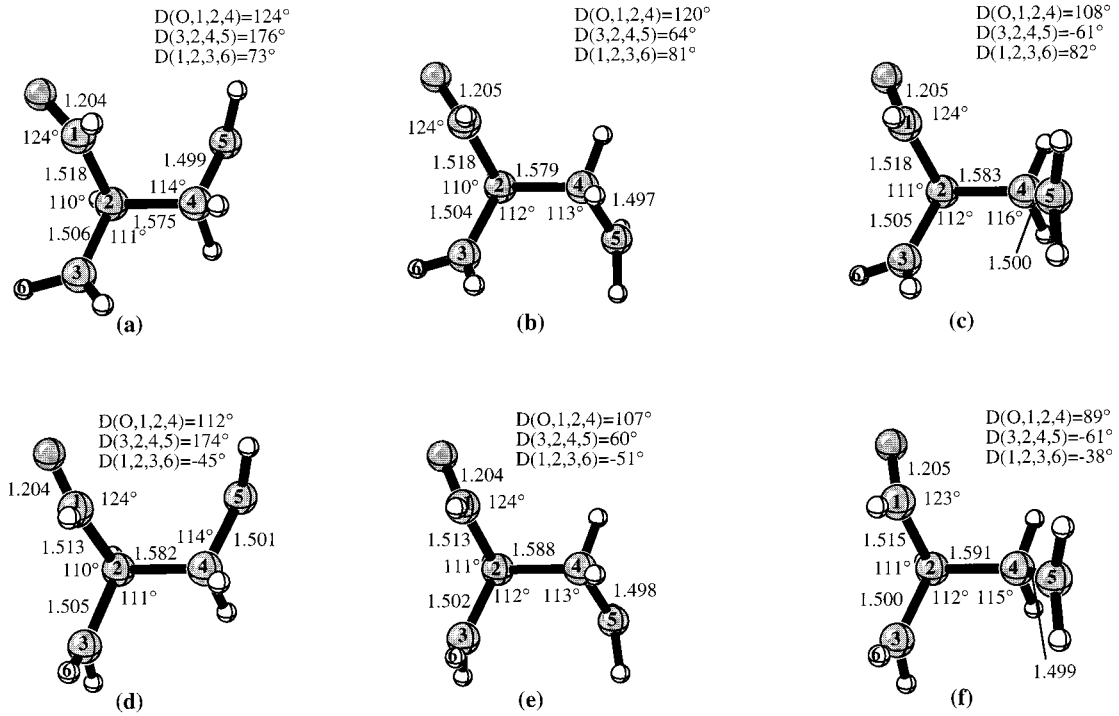

Figure 2. CASSCF(6,6)/6-31G* optimized $^3(\pi\pi^*)$ biradical intermediates formed after α-attack (bond lengths in Å and angles in deg): (a) *anti* biradical; (b) *gauche-out* biradical; (c) *gauche-in* biradical; (d) *anti* biradical after methylene twist; (e) *gauche-out* biradical after methylene twist; and (f) *gauche-in* biradical after methylene twist.

Results and Discussion

In this section the results of calculations carried out on the ground-state (S_0), triplet-state ($^3(\pi\pi^*)$ and $^3(n\pi^*)$), and excited singlet-state ($^1(n\pi^*)$) potential energy surfaces for the addition of ethylene to acrolein to form formylcyclobutane are presented. We will show that both the excited-state and the ground-state surface topologies influence product formation, as predicted by Weedon and co-workers.[10] The transition states on the excited-state surfaces determine the nature of the biradical intermediate

(22) Koseki, S.; Schmidt, M. W.; Gordon, M. S. *J. Phys. Chem.* **1992**, *96*, 10768.

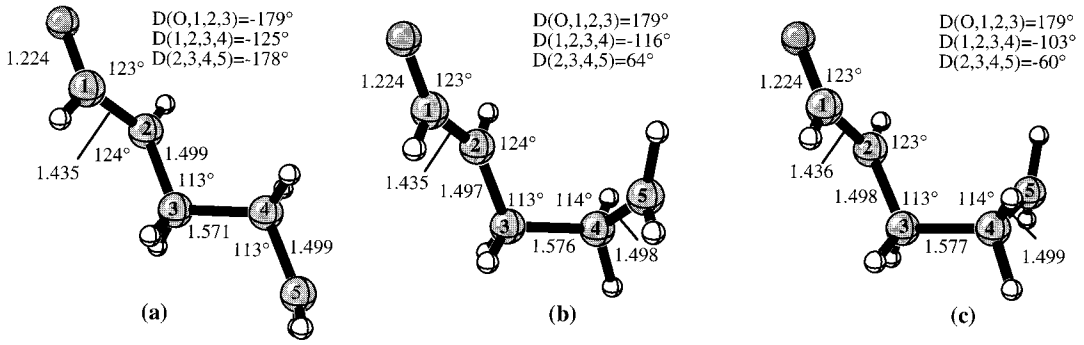

Figure 3. CASSCF(6,6)/6-31G* optimized $^3(\pi\pi^*)$ biradical intermediates formed after β-attack (bond lengths in Å and angles in deg): (a) *anti* biradical; (b) *gauche-in* biradical; and (c) *gauche-out* biradical.

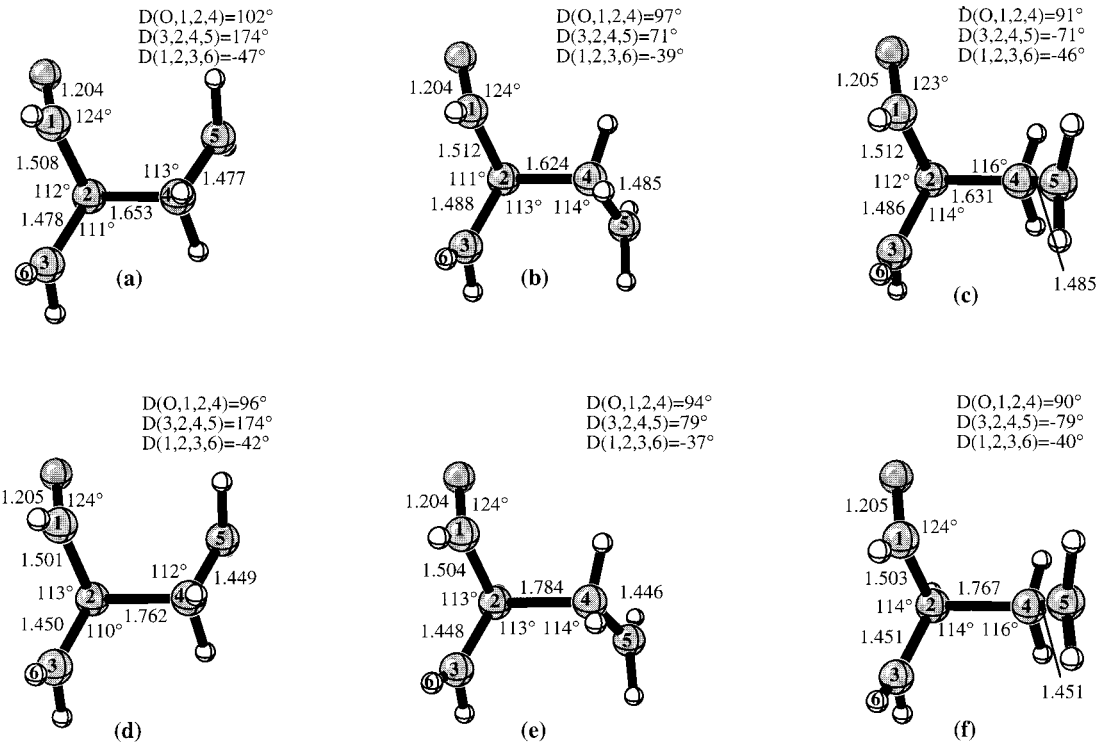

Figure 4. CASSCF(6,6)/6-31G* optimized S_0 biradical minima and dissociation transition structures for α-attack (bond lengths in Å and angles in deg): (a) *anti* biradical intermediate; (b) *gauche-out* biradical intermediate; (c) *gauche-in* biradical intermediate; (d) *anti* dissociation transition structure; (e) *gauche-out* dissociation transition structure; and (f) *gauche-in* dissociation transition structure.

Scheme 2

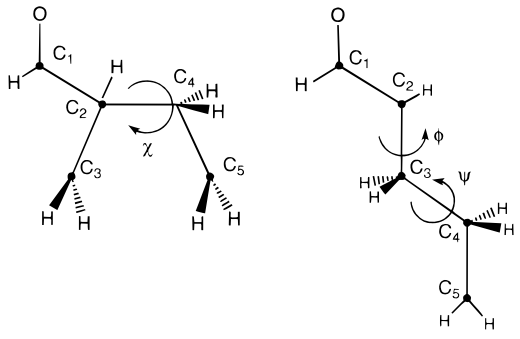

initially formed, while those on the ground-state surface control the competition between biradical ring-closure to form products and bond-cleavage back to reactants.

The optimized structures for the [2+2]-cycloaddition of $^3(\pi\pi^*)$ *s-trans*-acrolein to ethylene are shown in Figures 1−7, with the corresponding energetics given in Table 1. $^3(\pi\pi^*)$ *s-cis*-acrolein lies 0.5 kcal/mol higher in energy than *s-trans*-acrolein, and their potential energy surfaces are very similar. The transition state energies computed for the α- and β-attack of $^3(\pi\pi^*)$ *s-cis*-acrolein on ethylene differ by less than 0.5 kcal/mol from those computed for *s-trans*-acrolein, therefore the following discussion will focus on the results obtained for *s-trans*-acrolein. The energies for the *s-cis* structures can be obtained as Supporting Information.

The nomenclature used for labeling the structures for addition at the α-position of acrolein refers to the dihedral angle χ indicated in Scheme 2, where *anti* structures have an angle χ of approximately 180°, *gauche-out* structures have angles close to +60°, and *gauche-in* structures have angles of about −60°. The labeling used for the structures involved with addition at the β-position of acrolein is composed of two parts corresponding to the dihedrals ϕ and ψ. *Syn* structures have angles ϕ close to 0°, and *anti* structures have angles ϕ of approximately 180°. *Anti* and *gauche* structures about the dihedral angle ψ are defined as for χ except in this case *gauche-out* refers to structures with angles of −60° and *gauche-in* with angles of +60°.

The equilibrium minima on the ground-state, $^3(\pi\pi^*)$ state, $^3(n\pi^*)$ state, and $^1(n\pi^*)$ state surfaces of acrolein are identical

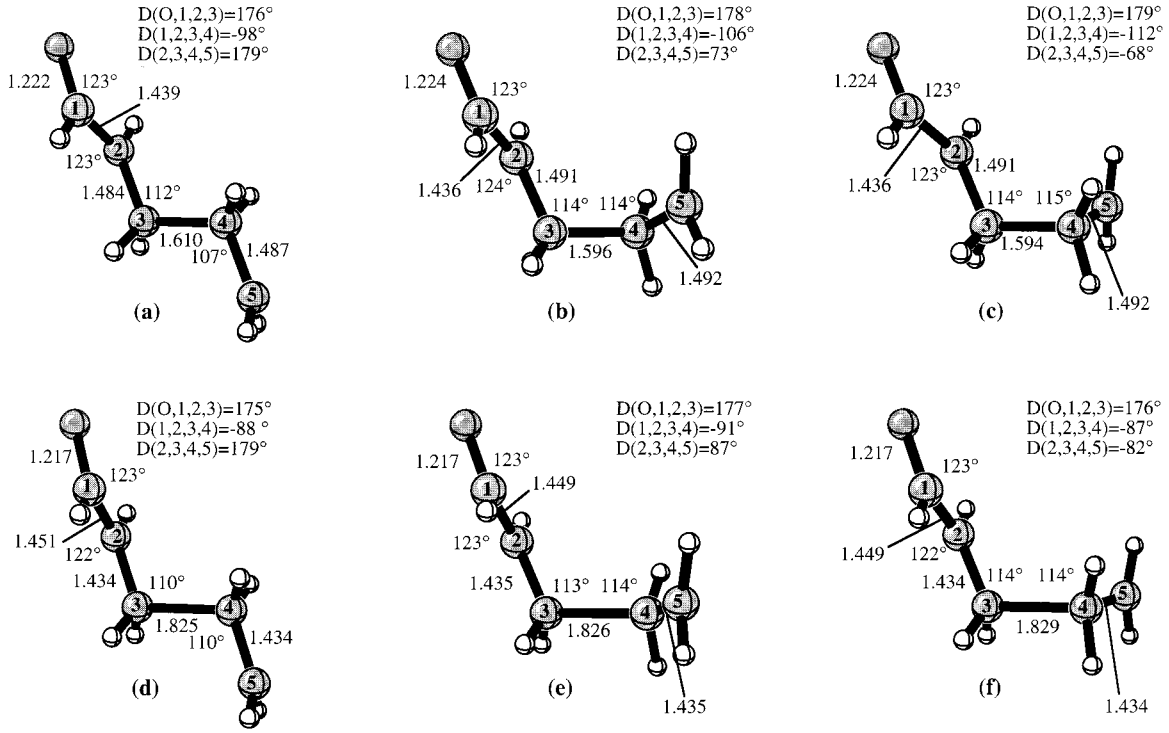

Figure 5. CASSCF(6,6)/6-31G* optimized S_0 biradical minima and dissociation transition structures for *β*-attack (bond lengths in Å and angles in deg): (a) *anti* biradical intermediate; (b) *gauche-in* biradical intermediate; (c) *gauche-out* biradical intermediate; (d) *anti* dissociation transition structure; (e) *gauche-in* dissociation transition structure; and (f) *gauche-out* dissociation transition structure.

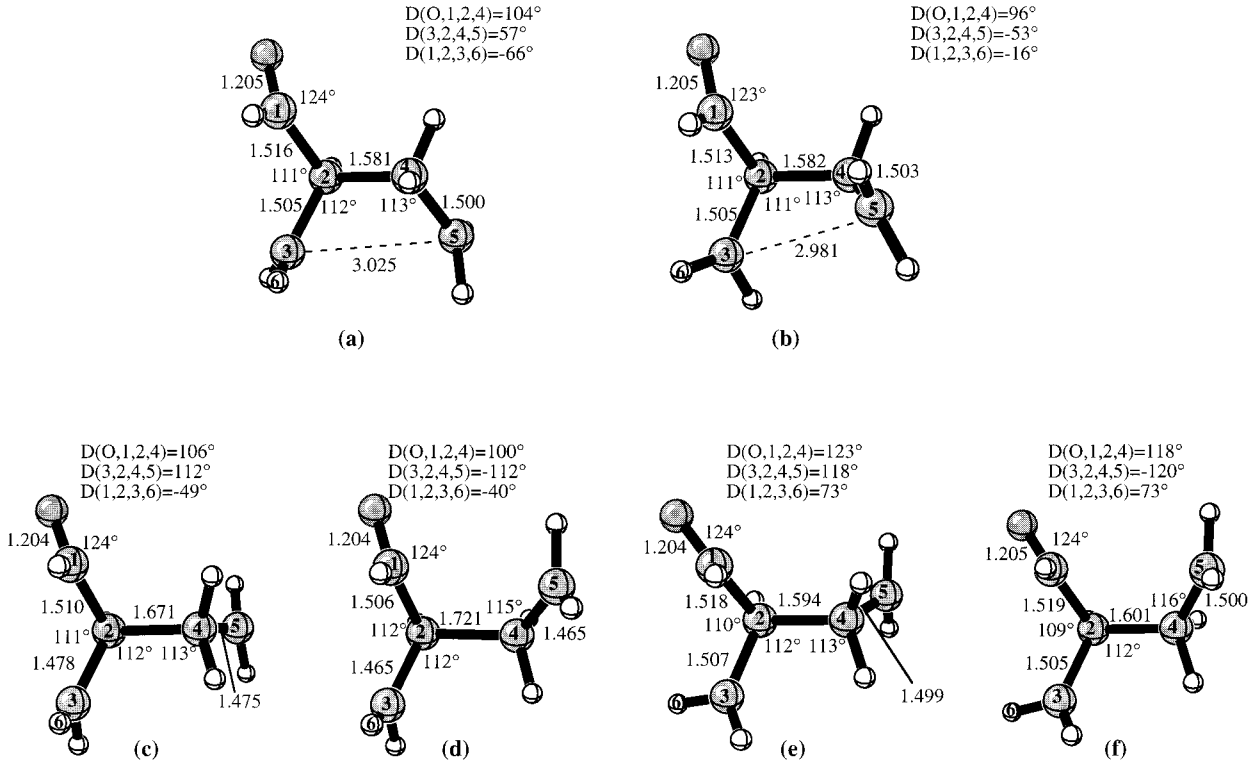

Figure 6. CASSCF(6,6)/6-31G* optimized transition structures for reaction from the α-biradicals (bond lengths in Å and angles in deg): (a) S_0 transition structure for ring-closure from *gauche-out* biradical; (b) S_0 transition structure for ring-closure from *gauche-in* biradical; (c) S_0 *anti/gauche-out* interconversion transition structure; (d) S_0 *anti/gauche-in* interconversion second-order saddle point; (e) $^3(\pi\pi^*)$ *anti/gauche-out* interconversion transition structure; and (f) $^3(\pi\pi^*)$ *anti/gauche-in* interconversion transition structure.

with those calculated by Reguero et al. and the energies are the same to within 0.5 kcal/mol.[8] The optimized geometries can be obtained as Supporting Information. At the geometry of the ground-state reactants the $^3(n\pi^*)$ state is the lowest excited state; the $^3(\pi\pi^*)$ and $^1(n\pi^*)$ states are some 4 and 5 kcal/mol higher in energy, respectively. However, if the geometries are allowed to relax, the $^3(\pi\pi^*)$ state falls below the $^3(n\pi^*)$ state and the triplet-sensitized reaction normally occurs from this state. The

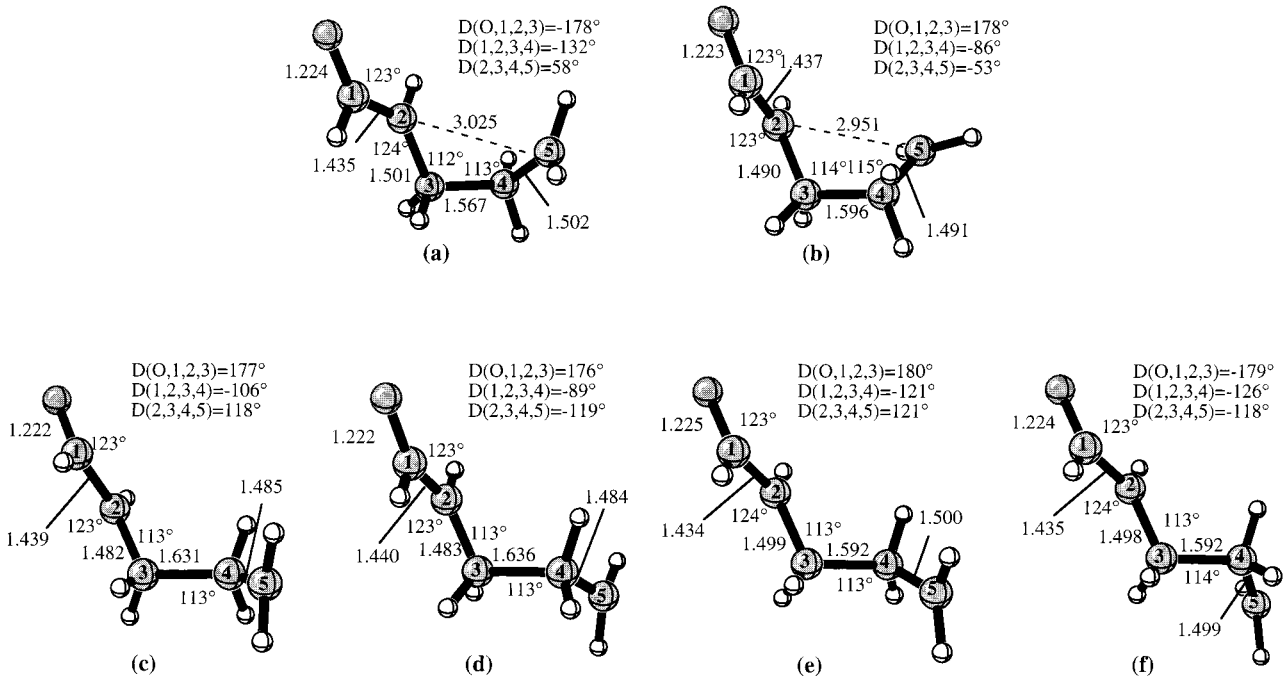

Figure 7. CASSCF(6,6)/6-31G* optimized transition structures for reaction from the β-biradicals (bond lengths in Å and angles in deg): (a) S_0 transition structure for ring-closure from *gauche-in* biradical; (b) S_0 transition structure for ring-closure from *gauche-out* biradical; (c) S_0 *anti/gauche-in* interconversion transition structure; (d) S_0 *anti/gauche-out* interconversion transition structure; (e) $^3(\pi\pi^*)$ *anti/gauche-in* interconversion transition structure; and (f) $^3(\pi\pi^*)$ *anti/gauche-out* interconversion transition structure.

$^3(\pi\pi^*)$ minimum is twisted and lies 60 kcal/mol above the ground-state reactant minimum, while the $^3(n\pi^*)$ minimum is planar and lies a further 9.2 kcal/mol higher in energy. These results are in good agreement with the UMP4-(SDTQ)/6-31G*//UMP2/6-31G* energies obtained previously,[9] which placed the $^3(\pi\pi^*)$ twisted minimum 9.9 kcal/mol below the planar $^3(n\pi^*)$ minimum. The geometries agree within 0.022 Å.

(i) The $^3(\pi\pi^*)$ and Ground-State Surfaces. The transition structures for both the α- and β-attack of $^3(\pi\pi^*)$ acrolein on ethylene are shown in Figure 1. The *anti* (Figure 1a) and *gauche* (Figures 1b and 1c) transition states for α-attack lie about 20 kcal/mol above the reactant minimum, with no preference between them. The bond length of the forming bond is 2.17−2.18 Å compared to the UHF/3-21G bond length of 2.10 Å. The three different modes of attack each lead to the formation of a 1,4-biradical intermediate (Figures 2a−c) where the new bond has shortened to around 1.58 Å. A twist of the β-carbon methylene in each case gives the conformers shown in Figures 2d−f. Of the two types of conformer, structures **2a** and **2b** are the most stable *anti* and *gauche-out* conformers, whereas **2f** is the most stable *gauche-in* conformer.

The energies of the transition structures for β-attack of ethylene to *s-trans*-acrolein (Figures 1d−g) range from 16.4 kcal/mol for attack *anti* to the C1−C2 bond to 17.4 and 17.5 kcal/mol for attack *syn* to the C1−C2 bond. These results indicate a 3−4 kcal/mol preference for β-attack which is considerably larger than the 0.3 kcal/mol preference predicted by the PMP3/6-31G*//UHF/3-21G calculations.[9] Each of the four modes of attack leads to one of three possible 1,4-biradical intermediates (Figures 3a−c) where the new C3−C4 bond length is around 1.57 Å and rotation about the C2−C3 bond has occurred. These biradical intermediates are some 10 kcal/mol more stable than those formed by α-attack. This preference is in agreement with the results of Erickson and Kahn[17] and arises from the delocalization of the radical center on C2 over the carbonyl group as reflected in the bond lengths of the C1−O (1.22 Å:1.20 Å) and C1−C2 (1.44 Å:1.51 Å) bonds relative to those for α-attack.

The triplet biradical minima (Figures 2d−f and 3a−c) are almost coincident and degenerate with minima on the ground-state surface (Figures 4a−c and 5a−c). The spin−orbit coupling (SOC) constants computed between the two surfaces at these minima are negligible (<0.1 cm^{-1}) in all cases. This is not surprising as the structures correspond to almost "perfect" biradicals; there is almost no interaction between the radical centers such that singlet and triplet states differ only by the relative spins of the two unpaired electrons. However, since the two surfaces parallel each other throughout this region there are a large range of geometries over which intersystem crossing can occur which will increase the probability of a transition to the ground-state surface.

Once on the ground-state surface, the biradicals can either dissociate to reform the reactants or close to form the cyclobutane product. The preferred pathway is found to depend considerably on whether the conformation of the biradical is *anti* or *gauche*. *Gauche* biradicals show a tendency to close to form products; *anti* biradicals, on the other hand, need to rotate to a *gauche* conformer before ring-closure can occur and therefore prefer to cleave back to reactants. This leads to the formation of a large number of biradicals that will not go on to form products and explains the results observed experimentally by Weedon and co-workers.[10]

The transition structures for dissociation from the ground-state α- and β-biradicals back to reactants are shown in Figures 4d−f and 5d−f. The barriers for dissociation from the α-biradicals are only 0.7 and 0.3 kcal/mol for the *gauche* conformers (Figures 4e and 4f, respectively) and the barrier for the *anti* conformer (Figure 4d) actually disappears after zero-point energy correction. The barriers for ring-closure from the *gauche-out* and *gauche-in* minima to form *cis*- or *trans*-formylcyclobutane are comparable, 0.3 (Figure 6a) and 0.8 kcal/mol (Figure 6b), respectively, indicating a small preference for ring-closure

Scheme 3

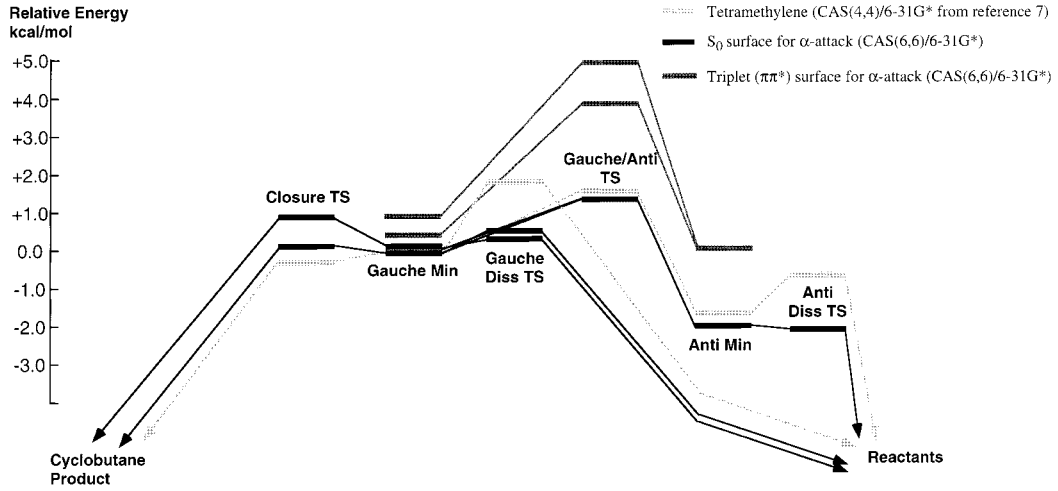

Scheme 4

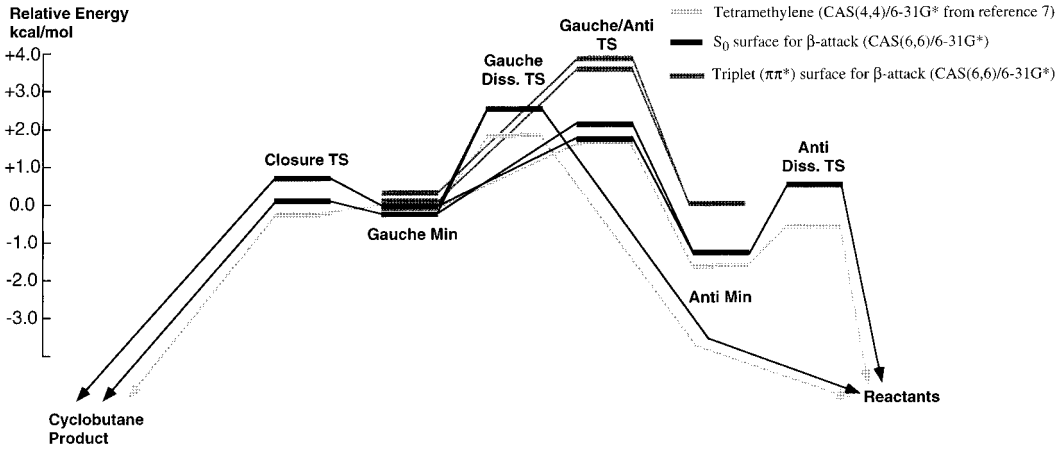

from the *gauche-out* biradical and a small preference for dissociation from the *gauche-in* biradical.[23]

In the case of the *anti* α-biradical (Figure 4a), dissociation is strongly favored over ring-closure which requires rotation about the newly formed C2−C4 bond to give one of the *gauche* conformers. The computed energies of the *anti/gauche* interconversion transition structures on the ground-state surface are approximately 3.4 kcal/mol for both conformers (Figure 6c,d).[24] The *anti/gauche* interconversion transition structures on the triplet surface leading from structure **2a** to **2b** and **2c** are higher in energy (3.7 kcal/mol (Figure 6e) and 4.8 kcal/mol (Figure 6f)). However, these are still well below the energy of the initial transition structure, so it is also possible that *anti/gauche* interconversion occurs before intersystem crossing to the ground-state surface.

A similar trend is observed for the *β*-biradicals. The energies of the transition structures for dissociation are more substantial than those of the α-biradicals: 1.8, 2.5, and 2.7 kcal/mol for the *anti* (Figure 5d), *gauche-in* (Figure 5e), and *gauche-out* (Figure 5f) transition structures, respectively. The competing barriers for ring-closure are only 0.1 (Figure 7a) and 0.8 kcal/mol (Figure 7b) for the *gauche* conformers, but some 3.0 (Figure 7c) and 3.4 kcal/mol (Figure 7d) for *anti/gauche* interconversion from the *anti* minimum. Therefore, again we would predict that the *gauche* biradicals will prefer to undergo ring-closure while the *anti* biradicals will prefer to fragment. The corresponding barriers for *anti/gauche* interconversion on the triplet surface are 3.8 (Figure 7e) and 3.5 kcal/mol (Figure 7f), therefore again there is the possibility of *anti/gauche* interconversion prior to intersystem crossing.

The competition between ring-closure and dissociation of the α- and *β*-biradicals formed in the addition of acrolein to ethylene is reminiscent of that observed for the tetramethylene biradical[7] and is expected to exist in many other 1,4-biradical systems. Comparisons of the tetramethylene potential energy surface obtained by Doubleday with the ground-state energies obtained for the α- and *β*-biradicals are shown in Schemes 3 and 4, respectively. The profiles for both α- and *β*-attack are remarkably similar to that of tetramethylene. The main differences between the α-biradical and tetramethylene (Scheme 3) are the barriers for dissociation which are about 1 kcal/mol lower in the enone system, such that fragmentation will compete more effectively with ring-closure from the *gauche* minima. In

(23) In Doubleday's paper (ref 7), three different transition states for ring-closure of tetramethylene to form cyclobutane are documented, corresponding to closure with two, one, or no methylene twists. In this work it was extremely difficult to converge these closure transition states as the surfaces are so flat with respect to these methylene torsions. Structures **6a** and **6b** could not be fully optimized (the forces were converged but the displacements were not converged). Both structures were obtained as second-order saddle points with two imaginary frequencies that correspond predominantly to symmetric and antisymmetric combinations of methylene torsions so that the energies may be slightly overestimated. Structures **7a** and **7b** correspond to ring-closure with one and no methylene torsions, respectively.

(24) Structures **6c** and **6d** could not be completely optimized (the maximum displacements did not converge). Structure **6d** was obtained as a second-order saddle point with small imaginary frequencies of 80 and 146 cm^{-1} corresponding to torsion around the newly formed bond and dissociation, respectively.

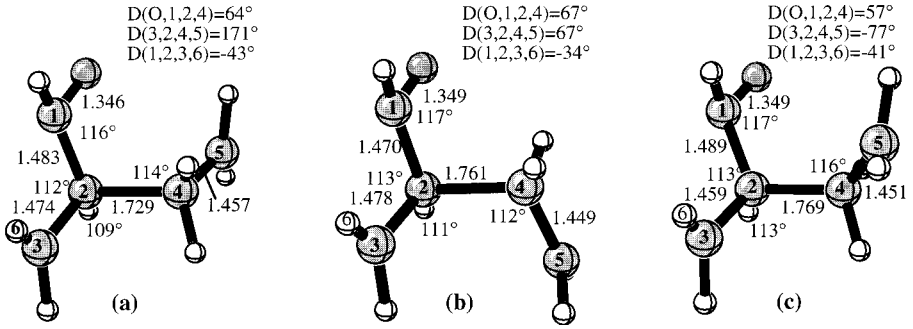

Figure 8. CASSCF(6,6)/6-31G* optimized $^3(n\pi^*)$ transition structures for α-attack (bond lengths in Å and angles in deg): (a) *anti* transition structure; (b) *gauche-out* transition structure; and (c) *gauche-in* transition structure.

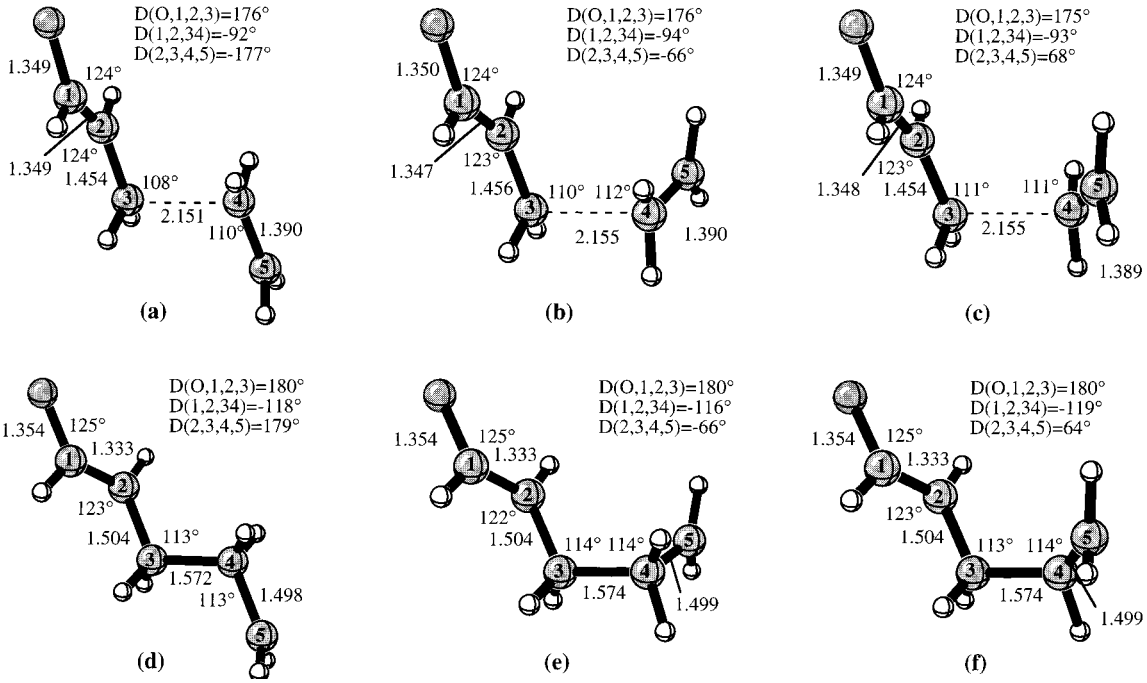

Figure 9. CASSCF(6,6)/6-31G* optimized $^3(n\pi^*)$ transition structures and CASSCF(8,7)/6-31G* optimized 1,6-biradical intermediates for β-attack (bond lengths in Å and angles in deg): (a) *anti* transition structure; (b) *gauche-out* transition structure; (c) *gauche-in* transition structure; (d) *anti* biradical; (e) *gauche-out* biradical; and (f) *gauche-in* biradical.

contrast, the dissociation transition structures from the β-biradicals are higher in energy than in the tetramethylene system (Scheme 4), leading to the formation of more cyclobutane product.

(ii) The $^3(n\pi^*)$ and $^1(n\pi^*)$ Surfaces. Efficient intersystem crossing ($^1(n\pi^*) \rightarrow {}^3(\pi\pi^*)$) and internal conversion ($^3(n\pi^*) \rightarrow {}^3(\pi\pi^*)$) occurs in acrolein at planar geometries and crossing points have been located previously for these processes.[8] However, in more constrained systems where the $^3(\pi\pi^*)$ state is unable to twist, the $n\pi^*$ states may play a role. The $^1(n\pi^*)$ and $^3(n\pi^*)$ surfaces parallel each other from the region of the reactants to the biradical regions. The transition structures and biradical intermediates for α- and β-attack on the $^3(n\pi^*)$ surface were located, and single-point energy calculations on the $^1(n\pi^*)$ surface were computed at these points. The results indicate that the $^1(n\pi^*)/^3(n\pi^*)$ energy difference at the $^3(n\pi^*)$ reactants is only 2 kcal/mol; this energy difference decreases as the new bond forms and the two radical centers become more separated until the biradical region is reached and the two surfaces become degenerate.

The transition structures for $^3(n\pi^*)$ α-attack (Figure 8a−c) lie some 40 kcal/mol above the corresponding $^3(\pi\pi^*)$ structures (see Table 2) as they involve decoupling both π systems in the enone molecule. Therefore α-attack is very unlikely to occur from the $n\pi^*$ states. $^3(n\pi^*)$ attack by the β-carbon, on the other hand, gives rise to transition structures (Figures 9a−c) which lie only 3 kcal/mol above the transition structures for α-attack from the $^3(\pi\pi^*)$ surface. The $^1(n\pi^*)$ energies at these transition structures are a further 2 kcal/mol higher in energy. Therefore reaction from the $n\pi^*$ surface, if it occurs, is expected to occur via β-attack.

The transition states lead to 1,6-biradicals (Figures 9d−f) where one unpaired electron is on C5 and the other is on the oxygen atom, with a new π bond between C1 and C2. The $^3(n\pi^*)$ biradicals could only be optimized in a CAS(8,7) active space using state-averaged orbitals as the $^3(\pi\pi^*)$ surface is too close in energy at these structures. Internal reaction coordinate (IRC) calculations with a CAS(6,6) active space initiated at the transition structures all terminated in the region of these biradicals, although in each case the calculation stopped because of problems converging the geometry at C3−C4 bond lengths of less than 1.6 Å. The energies of the last converged points of the IRCs are also given in Table 2.

State-averaged calculations between the $^1(n\pi^*)$ and ground-state surfaces at the biradical minima indicate that the $^1(n\pi^*)$ state is degenerate with the $^3(n\pi^*)$ state at these structures, while

Table 2. Energies Computed at the CAS/6-31G* Level for the Addition of $^3(n\pi^*)$ and $^1(n\pi^*)$ *s-trans*-Acrolein to Ethylene

structure	figure no.	state	CAS(6,6) E_{rel}, kcal/mol	CAS(6,6) ZPE, kcal/mol	CAS(6,6) E_{rel} + ZPE, kcal/mol	CAS(8,7) E_{rel}, kcal/mol
S_0 reactants		S_0				−69.2
		$^3(\pi\pi^*)$				20.3
		$^3(n\pi^*)$				16.1
		$^1(n\pi^*)$				21.5
$^3(n\pi^*)$ reactants		$^3(n\pi^*)$	0.0	71.8	0.0	0.0
		$^3(\pi\pi^*)$				8.8[a,b]
		$^3(n\pi^*)$				1.2[a,b]
		$^1(n\pi^*)$				3.4
$^1(n\pi^*)$ reactants		$^1(n\pi^*)$				3.2
α-attack						
anti TS	8a	$^3(n\pi^*)$	58.0	73.1	59.3	58.3
		$^1(n\pi^*)$				60.9
gauche-out TS	8b	$^3(n\pi^*)$	58.8	72.8	59.7	59.0
		$^1(n\pi^*)$				60.2
gauche-in TS	8c	$^3(n\pi^*)$	61.3	72.8	62.3	61.5
		$^1(n\pi^*)$				65.2
β-attack						
anti TS	9a	$^3(n\pi^*)$	21.6	73.7	23.5	23.2[a,b]
		$^3(\pi\pi^*)$				16.8[a,b]
		$^1(n\pi^*)$				25.3[c]
		S_0				−11.6[c]
gauche-out TS	9b	$^3(n\pi^*)$	22.1	73.4	23.7	23.8[a,b]
		$^3(\pi\pi^*)$				16.6[a,b]
		$^1(n\pi^*)$				25.7[c]
		S_0				−9.5[c]
gauche-in TS	9c	$^3(n\pi^*)$	21.8	73.4	23.4	23.5[a,b]
		$^3(\pi\pi^*)$				16.3[a,b]
		$^1(n\pi^*)$				25.5[c]
		S_0				−9.9[c]
anti min	9d	$^3(n\pi^*)$	−1.2[d]			−1.1[b]
		$^3(\pi\pi^*)$				−12.3[b]
		$^1(n\pi^*)$				−1.1[c]
		S_0				−12.9[c]
gauche-out min	9e	$^3(n\pi^*)$	−0.4[d]			−0.6[b]
		$^3(\pi\pi^*)$				−11.9[b]
		$^1(n\pi^*)$				−0.6[c]
		S_0				−12.2[c]
gauche-in min	9f	$^3(n\pi^*)$	−0.5[d]			−0.8[b]
		$^3(\pi\pi^*)$				−12.2[b]
		$^1(n\pi^*)$				−0.8[c]
		S_0				−12.0[c]
anti CI	10a	$^3(n\pi^*)$				15.0[b,e]
		$^3(\pi\pi^*)$				14.9[b,e]
		$^1(n\pi^*)$				15.0[c]
		S_0				14.9[c]
gauche CI	10b	$^3(n\pi^*)$				15.1[b,e]
		$^3(\pi\pi^*)$				14.9[b,e]
		$^1(n\pi^*)$				15.4[c]
		S_0				14.3[c]

[a] Single point calculation at CAS(6,6) geometry. [b] Computed with state-averaged orbitals equally weighted over the two triplet states. [c] Computed with state-averaged orbitals equally weighted over the two singlet states. [d] Taken from the last optimized point of an IRC. [e] Displacements not converged.

the $^3(\pi\pi^*)$ state is degenerate with the ground-state surface and lies some 11 kcal/mol lower in energy. Two $^3(n\pi^*)/^3(\pi\pi^*)$ crossing points were located in the vicinity of these biradicals (Figure 10) although these could not be completely optimized (the forces converged but the displacements did not converge). These occur at geometries where considerable rotation about the C2−C3 bond has occurred such that the C1−C2 bond is nearly *cis* to the C3−C4 bond and the C−O bond length has increased to 1.39−1.40 Å. At both points there is a four-level degeneracy with the singlet surfaces. The spin−orbit coupling constants computed between the $^1(n\pi^*)/^3(\pi\pi^*)$ and $^3(n\pi^*)/S_0$ surfaces are both 39 (*anti*) and 49 cm^{-1} (*gauche*) implying efficient intersystem crossing if these points are accessed. However, these crossing points lie some 16 kcal/mol above the biradical minima such that, at least in the parent system, intersystem crossing and internal conversion are expected to be slow in this region.

Therefore, on the basis of our calculations it appears that there are two $^1(n\pi^*)/^3(n\pi^*)/^3(\pi\pi^*)$ crossing regions. In the acrolein system, both intersystem crossing and internal conversion before the transition state region leading to $^3(\pi\pi^*)$ acrolein is expected to be more efficient than decay to the ground-state surface in the biradical regions. However, in other, more constrained, enone systems the topology of the crossing regions may be different and the reaction may proceed on the $n\pi^*$ surfaces into the biradical regions, followed by internal conversion or intersystem crossing at the four-level degenerate crossing points.

Conclusions

The [2+2]-photocycloaddition of $^3(\pi\pi^*)$ α,β-enones and alkenes is controlled by both the triplet- and ground-state surface topologies. The twisted structure of the $^3(\pi\pi^*)$ minimum of *s-trans*-acrolein gives rise to three different modes of α-attack

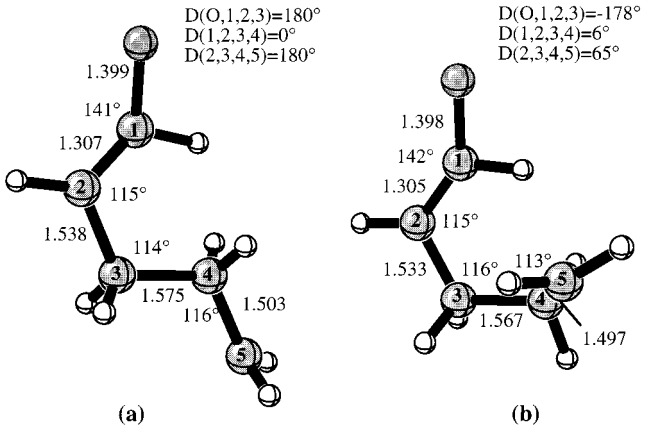

Figure 10. CASSCF(8,7)/6-31G* optimized $^3(n\pi^*)/^3(\pi\pi^*)$ crossing points (bond lengths in Å and angles in deg): (a) *anti* conical intersection; and (b) *gauche* conical intersection.

and four different modes of β-attack. Transition states on the triplet surface control the ratio of α- versus β-attack (with a 3−4 kcal/mol preference for β-attack in the parent system), as well as the conformation (*anti* or *gauche*) of the triplet biradical formed. All of the triplet biradical intermediates formed can undergo intersystem crossing to the ground-state surface. Intersystem crossing is not particularly efficient as the spin−orbit coupling is small, but its probability is increased by the fact there are minima on both surfaces which parallel each other in these regions.

Once on the ground-state surface, the molecule can either close to form the cyclobutane product or dissociate to reform the reactants. The conformation of the biradical determines which of these processes will be preferred, explaining the large discrepancy observed between the HH:HT ratios of the biradicals and the products in the radical trapping experiments.[10] The results indicate that for ethylene, the *anti* biradical formed by β-attack of the $^3(\pi\pi^*)$ enone will form most rapidly, but this will mainly dissociate (Scheme 4). *Gauche* biradicals will be formed more slowly and mainly undergo ring-closure. The same behavior is expected of reactions of enones with electron-deficient alkenes, with the formation of HH products.

Previous investigations[9] suggest that electron-rich alkenes will be attacked by the electrophilic α-radical of the $^3(\pi\pi^*)$ enone at the less-substituted alkene terminus. Our results predict that both *anti* and *gauche* biradicals will be formed to a similar extent. Scheme 3 suggests that these biradicals will mainly dissociate, with slow formation of cyclobutanes occurring from the *gauche* α-biradical, leading to HT products.

Finally, reaction from the $n\pi^*$ surfaces is only expected to take place via β-attack as the barriers for α-attack are so much higher in energy. Attack of $^3(n\pi^*)$ or $^1(n\pi^*)$ acrolein on ethylene leads to the formation of 1,6-biradicals. Two $^1(n\pi^*)/^3(n\pi^*)/^3(\pi\pi^*)$ crossing regions exist, the first in acrolein itself and the second close to the biradicals. For the parent system described here, the biradical crossing points occur some 16 kcal/mol above the $^3(n\pi^*)$ biradical minima such that intersystem crossing or internal conversion to the $^3(\pi\pi^*)$ surface is expected to occur before the transition state region. However, with substituted enones, reaction may proceed on the $n\pi^*$ surfaces with decay to the ground-state surface occurring close to the biradical minima at a point of four-level degeneracy.

Acknowledgment. We are grateful to the National Science Foundation for financial support of this research. This work was partially supported by the National Computational Science Alliance and utilized the ncsa sgi/cray powerchallenge array. We also thank the San Diego Supercomputing Center and the UCLA Office of Academic Computing for computational resources. S.W. thanks the Royal Society for a NATO Fellowship and the Fulbright Commission for a scholarship during her time at UCLA. She would also like to thank the Violette and Samuel Glasstone Trust for a fellowship at Oxford University. L.G. is grateful to the Ministerio de Educación y Cultura (Spain) for a traveling grant to visit the group of M.A.R.

Supporting Information Available: A table containing the computed energies of the transition structures for the attack of $^3(\pi\pi^*)$ *s-cis*-acrolein on ethylene and a figure containing the optimized structures of the reactants and products (PDF). This material is available free of charge via the Internet at http://pubs.acs.org.

JA0006595